Improvement of photorefractive properties of proton-exchanged LiTaO₃ waveguides

S.M. Kostritskii[1], D. Kip[2], E. Krätzig[2]

[1] Department of Physics, Kemerovo State University, 650043 Kemerovo, Russia
(Fax: +7-3842/525383; E-mail: root@chsb.kemgu.kemerovo.su)
[2] Fachbereich Physik, Universität Osnabrück, D-49069 Osnabrück, Germany
(Fax: +49-541/9692670; E-mail: dkip@physik.uni-osnabrueck.de)

Abstract. Photorefractive planar waveguides in LiTaO₃ are fabricated by both a proton exchange and a successive copper exchange. The influence of different fabrication steps on the refractive index profile and optical absorption is investigated. The holographic efficiency is determined together with the dark- and photo-conductivity. We show that the photorefractive properties of proton-exchanged LiTaO₃ waveguides are considerably improved by the additional copper exchange. It is established that the holographic efficiency depends on the copper content, the phase of the proton-exchanged layer and the light intensity.

PACS: 42.40; 42.82; 78.20

LiTaO₃ crystals are of increasing interest for the fabrication of integrated optical devices because of their excellent properties [1]. In contrast to bulk samples, in waveguides it is easy to obtain high light intensities with moderate input power; large photorefractive effects can be observed. Therefore photorefractive waveguides may be used as integrated optical switches, sensors or memory cells [2]. However, the common fabrication methods by indiffusion processes require some technological efforts for LiTaO₃ as the Curie temperature is at about 620 °C and indiffusion at high temperatures requires additional poling [3]. At the same time, there is a quick, technologically easy method for the production of photorefractive waveguides, originally developed for LiNbO₃: a combined proton and copper exchange [4, 5] at rather low temperatures. By the additional copper exchange the steady-state diffraction efficiency of holographic gratings in proton-exchanged LiNbO₃ waveguides was increased from 0.01 to 65% [5]. Evidently this method of a combined proton and copper exchange is also of great interest for LiTaO₃. In this paper we present the first results on the photorefractive properties of proton- and copper–exchanged planar LiTaO₃ waveguides.

1 Sample preparation and characterization

1.1 Fabrication of the waveguides

For the fabrication of the waveguides we use polished z-cut LiTaO₃ substrates of nearly congruently melting composition. The substrates are subjected to the following treatments: (1) proton exchange in pure molten benzoic acid at 240 °C for 8 hours, (2) weak annealing in dry air in two steps: first, at 265 °C for 1 hour and, second, at 295 °C for 45 min (this annealing treatment was found to enlarge the amplitude of the extraordinary refractive index profile and to avoid the marked long-term instability of proton-exchanged LiTaO₃ waveguides [6]), (3) copper exchange in molten benzoic acid mixed with 7 wt. % copper acetate at 249 °C for 30 to 90 min (water, usually present in copper acetate, is removed from the mixture by a separate technological step between the mixture preparation and the sample treatment), (4) annealing in air at 350 °C for 1 to 6 hours.

1.2 Copper content

The copper content in the waveguides is determined by measuring the optical absorption of the samples in the UV and the visible region with the help of a Cary 17D spectrometer. We observe the appearance of a new band in the absorption spectrum at about 4 eV which increases with the duration of the copper exchange, Fig. 1. This band is observed near the edge of the fundamental absorption (4.5 eV). The position of the new band agrees with the data in [7] on the optical spectra of Cu:LiTaO₃ waveguides obtained by ionic exchange in molten copper (II) salts. This band is assumed to be directly connected with Cu complexes and its intensity to be proportional to the copper content in the doped waveguides.

1.3 Effective refractive indices

The effective refractive indices n_{eff}^i of the TM$_i$ modes are measured by the method of prism-coupling (dark line
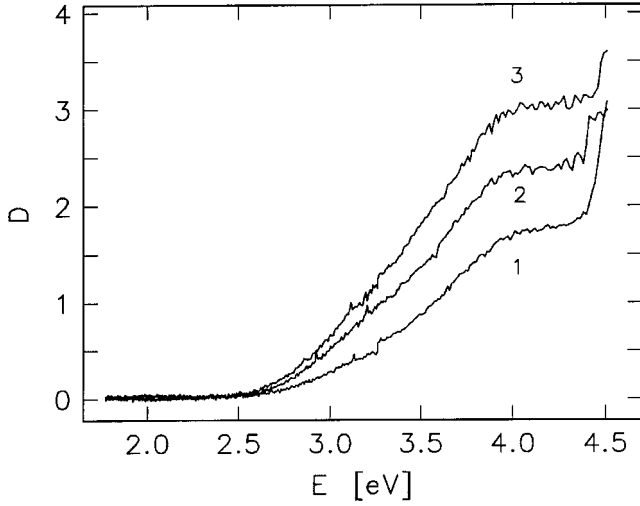
Fig. 1. Difference spectra of the copper-exchanged waveguides and the undoped waveguide LT1: the optical density D ($=^{10}\log I/I_0$) versus photon energy E is shown: *Curve 1* sample LT2, copper exchange time $t_{ce} = 30$ min; *curve 2* sample LT3, $t_{ce} = 60$ min; *curve 3* sample LT4, $t_{ce} = 90$ min

Table 1. Values of the increment δn_e of the extraordinary index at the surface for different annealing times t_a at 350 °C for the waveguides LT1 (no copper exchange), LT2 (copper exchange time $t_{ce} = 30$ min), LT3 ($t_{ce} = 60$ min) and LT4 ($t_{ce} = 90$ min). The measuring accuracy is ±0.0008. For comparison the optical density D at 4 eV is also given

sample	D(4 eV)	t_a [h]		
		1	2	3
LT1	0	0.0285	0.0245	0.0229
LT2	1.00	0.0352	0.0300	0.0285
LT3	1.75	0.0426	0.0333	0.0323
LT4	2.33	0.0458	0.0389	0.0353

Remark: Before annealing all waveguides have the values δn_e of 0.0225 ± 0.0008.

spectroscopy) at $\lambda_0 = 514.5$ nm. From the effective refractive indices the profile of the extraordinary refractive index is reconstructed by the use of an inverse WKB method. Furthermore, we measure the IR absorption in the region of the OH-vibration band around 3500 cm^{-1} using a Specord M80 spectrometer with the aim to determine the phase of the Li$_{1-x}$H$_x$TaO$_3$ layers using data from [8,9]. The IR absorption spectra of all waveguides, both undoped and copper-doped, correspond to a pure paraelectric β-phase of Li$_{1-x}$H$_x$TaO$_3$ after fabrication. These waveguides have a step-like profile with a depth of (2.4 ± 0.2) μm and an increment δn_e of the extraordinary refractive index δn_e of (0.0225 ± 0.0008). In all waveguides only two TM modes can be excited before annealing.

After annealing at 350 °C, in all waveguides five TM modes can be excited with different effective refractive indices. The analysis of the refractive index profiles of the annealed waveguides yields a nearly Gaussian form, and the value of δn_e near the surface is strongly increased compared with the initial stage after proton exchange. Moreover, the magnitude of the increase of the refractive index clearly grows with increasing copper content in the waveguides, see Table 1.

1.4 Hydrogen content

In Li$_{1-x}$H$_x$TaO$_3$ waveguides different phases occur [8]. For large x, $x > x_\beta$, there exists the above mentioned paraelectric β-phase. For small x, $x < x_\alpha$, the crystal remains in the ferroelectric α-phase which corresponds to the structure of LiTaO$_3$. For $x_\alpha < x < x_\beta$ the crystal is composed of a mixture of the two phases. Here x_α and x_β characterize the boundary

between the pure α- and the mixed $(\alpha + \beta)$-phase and between the pure β- and the mixed $(\alpha + \beta)$-phase, respectively.

The IR spectra of our annealed waveguides are typical for a mixed $(\alpha + \beta)$-phase of Li$_{1-x}$H$_x$TaO$_3$ [6,8,9]. The comparison of our data and that of Ref. [8] indicates that the near-surface part of our waveguide LT1 which is annealed for 1 hour at 350 °C, corresponds to $x \approx x_\beta \approx 0.6$. With increasing depth (measured from the surface), x decreases until for $x < x_\alpha$ the pure α-phase exists.

In previous investigations [6,8] a linear relation between the refractive index increment δn_e and the proton concentration x for well annealed waveguides has been established. Consequently, for the determination of x in different propagation depths of the TM modes in the annealed undoped waveguides we set

$$(n_e + \delta n_e^\beta) - n_{eff}^i = A(x_\beta - x)\,, \tag{1}$$

where $n_e = 2.2097$ is the extraordinary refractive index for the LiTaO$_3$ substrate, δn_e^β is the increment induced by the proton exchange at $x = x_\beta \approx 0.6$ (see above) and A is a constant. To obtain δn_e^β and A we use the following arguments. The near-surface part of waveguide LT1 annealed for 1 hour at 305 °C corresponds to $x \approx x_\beta$ and for this reason the value of δn_e at the surface ($= 0.0285$, Table 1) is approximately equal to δn_e^β. Furthermore, near the substrate ($x \to 0$) we have $n_{eff}^i \to n_e$ and then we get from Eq.(1): $A = \delta n_e^\beta / x_\beta$. Thus we obtain the following estimation for the hydrogen concentration x:

$$x = 21.053(n_{eff}^i - 2.2097)\,. \tag{2}$$

Note, this relation is fulfilled only for the values of the effective refractive indices n_{eff}^i of different TM$_i$ modes (measured at $\lambda_0 = 514.5$ nm) of annealed proton-exchanged waveguides without copper exchange. For annealed copper-doped waveguides we have contributions to the refractive index change resulting from hydrogen and copper. We assume $n_{eff}^i = n_e + \delta n_e^H(d) + \delta n_e^{Cu}(d)$, where $\delta n_e^H(d)$ and $\delta n_e^{Cu}(d)$ are the contributions of hydrogen and copper, respectively, at the propagation depth d for a given TM$_i$ mode. At first we determine the propagation depth of a TM$_i$ mode and then

$n_e + \delta n_e^H(d)$ is derived from the profile of the undoped waveguide. This value has to be used in (2) instead of n_{eff}^i to obtain the hydrogen concentration x of copper-doped waveguides.

1.5 Waveguide transparency

We measure the relative change of the waveguide transparency with the help of two rutil prisms which couple light into and out of the waveguide. The distance between the coupling points of these prisms is 4.5 mm. The ratio of output power to input power for the excitation of different TM_i modes indicates that the optical losses are similar for the TM_2, TM_3 and TM_4 modes in all waveguides annealed for a time not longer than 3 hours. The optical losses for the TM_0 and TM_1 modes are much higher which is caused mainly by the growth of optical absorption by Cu-defects, as the overlap of the intensity distribution of these modes with the copper profile is much larger than that for the TM_2, TM_3 and TM_4 modes. This conclusion about the difference in the overlap with the copper profile is a direct consequence of the sharp decrease of the copper-induced changes of n_{eff} when comparing the modes TM_1 and TM_2. However, the dependence of the transparency on the annealing time is non-monotonic: In all waveguides, both undoped and copper-doped, annealed for 2 h at 350 °C the transparency is much smaller (approximately by a factor of 3) than for annealing times of 1 or 3 hours. This anomaly is connected with special peculiarities of annealed proton-exchanged $LiTaO_3$ waveguides and will be discussed in the next section.

2 Investigation of photorefractive properties

2.1 Holographic method

To investigate light-induced refractive index changes Δn, holographic gratings are written and erased in planar $LiTaO_3$ waveguides (+c face) utilizing an argon-ion laser (wavelengths of 457, 488 and 514.5 nm). For this purpose two slightly focused beams are coupled into and out of the waveguide using two rutile prisms. Depending on the angle the light enters the prism, different extraordinarily (e) polarized modes (TM) are excited. The recording of holographic gratings in z-cut $LiTaO_3$ waveguides with extraordinarily polarized beams is possible only by using a special writing mechanism [10] that is based on photovoltaic currents and has no equivalent in bulk samples. In the experimental set-up two modes intersect at an angle of $2\Theta = 10°$, and the interaction length in the waveguides is about 1.5 mm. During the build-up of the refractive index grating, the diffraction efficiency η is measured as a function of time by blocking one of the beams for a short moment (50 ms) and measuring the ratio of diffracted and total light intensity of the outcoupled beams. When the saturation value of diffraction efficiency η^s is reached, one of the beams is switched off, and the continuous decrease of the diffracted light intensity indicates the decay of the grating during readout. Recording and erasure of holographic gratings are well described by mono-exponential laws:

$$\eta(t) = \eta^s(1 - e^{-t/\tau}), \quad \text{and} \quad \eta(t) = \eta^s e^{-t/\tau}, \tag{3}$$

where t denotes the time of recording and erasure. From the time constant τ of erasure and the relation $\eta \sim (\Delta n)^2$ we deduce the conductivity, $\sigma = \epsilon\epsilon_0/2\tau$.

2.2 Saturation value of efficiency

In non-annealed (or in weakly annealed) waveguides, both undoped and copper-doped, we do not observe holographic grating recording at any level of input power P_{in} (the maximum value of P_{in} in our investigations is 1.0 W, but the coupling efficiency is only about 1%) for all lines of the argon-ion laser. However, after annealing in air at 350 °C for 1 hour, effective writing of phase holograms becomes possible: An increase of η with increasing light power P_{in} occurs in all copper-doped waveguides, in contrast to undoped waveguides, see Fig. 2. The maximum value $\eta^s(max)$ and the slope of the dependence $\eta(P_{in})$ at very small input power clearly grows with increasing copper content in the waveguides after the same degree of annealing.

The value of $\eta^s(max)$ for the undoped waveguide LT1 at any degree of annealing does not exceed 0.005%. This means that copper exchange increases the diffraction efficiency of the photorefractive holograms written with TM_4 modes by a factor of up to thousand. However, there is a strong difference between different TM modes. The value of $\eta^s(max)$ at $\lambda_0 = 488$ nm for all annealed waveguides is reached using two TM_4 modes for writing. These are the highest guided modes that can be excited in the waveguides. For TM_3 modes, η^s is smaller, but holographic recording is rather effective, too (see Table 2). A different behaviour is observed using TM_2 modes; here holographic writing becomes possible only after annealing at 350 °C for a long time (3–6 hours) and η^s is only 0.03%. We do not succeed in observing holographic recording for TM_0 and TM_1 modes in our samples.
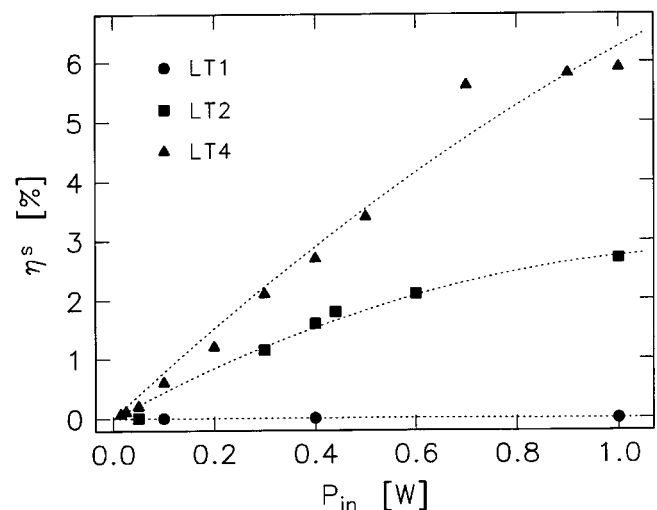
Fig. 2. Dependence of the steady state diffraction efficiency η^s on input power P_{in} in planar Cu:H:$LiTaO_3$ waveguides with different times t_{ce} of copper exchange, annealed at 350 °C for 1 h: LT1, $t_{ce} = 0$; LT2, $t_{ce} = 30$ min; LT4, $t_{ce} = 90$ min. The values are obtained using the TM_4 modes at $\lambda_0 = 488$ nm and the measuring accuracy is about 15%

Table 2. Saturation value of diffraction efficiency (in %) at the highest input power P_{in} of 1.0 W as a function of annealing time t_a for different TM modes of sample LT2 at $\lambda_0 = 488$ nm. The measuring accuracy is about $\pm 15\%$

Modes	t_a [h]			
	1	2	3	6
TM$_4$	2.7	0.12	1.1	4.2
TM$_3$	1.4	0.08	0.6	1.7
TM$_2$	0	0	0.01	0.03
TM$_1$	0	0	0	0
TM$_0$	0	0	0	0

The investigation of η^s for different TM$_i$ modes with $i \geq 2$ (Table 2) points to a strong influence of the hydrogen concentration (that decreases with increasing propagation depth of a mode) on the efficiency of holographic recording. This dependence is much stronger than the expected effect of the degradation of the electrooptic effect caused by the proton exchange as the corresponding electrooptic coefficient r_{33} is proportional to $(x_\beta - x)$ [8], and x has small values (< 0.3) for TM$_2$, TM$_3$ and TM$_4$ modes in our annealed LiTaO$_3$ waveguides. For small diffraction efficiencies $\eta^s < 10\%$, the following relationship is fulfilled [5, 11]:

$$\eta \sim (r_{33})^2 , \tag{4}$$

and hence, from the x values for TM$_2$ and TM$_4$ modes, we may expect a decrease of η^s by a factor of 3 to 3.5 when changing from the TM$_4$ to the TM$_2$ mode. But the experimental values of η^s differ by more than two orders of magnitude (see Table 2).

In our opinion the magnitude of η^s depends on the phase of the waveguiding layer, which again depends on its depth. It is known from [8] that the phase of proton-exchanged LiTaO$_3$ is characterized by a sharp change at a certain threshold value x_t of the hydrogen concentration. In accordance with data obtained by dark line spectroscopy, we find that x_t has the value of about $0.25 - 0.27$, derived from (2) and the effective refractive indices of TM$_2$ modes in different waveguides. We assume that for waveguides annealed for 1 and 2 hours at $350\,^\circ$C, the propagation depths of TM$_2$ modes correspond to the case $x \geq x_t$, and after annealing for 3 and 6 hours the condition $x < x_t$ is fulfilled for the depths of these modes. Evidently, the value of x_t must be near x_α in the phase diagram of Li$_{1-x}$H$_x$TaO$_3$. The differences between the values of η^s for TM$_2$, TM$_3$ and TM$_4$ modes in any waveguide may be described in a good approximation by the relation:

$$\eta^s \sim (x_\beta - x)^2 (x_t - x)^2 . \tag{5}$$

Therefore, a further increase of the photorefractive effect in copper-doped proton-exchanged LiTaO$_3$ waveguides may be expected either for strongly annealed samples or for samples fabricated by a combined proton and copper exchange in a special mixture with strongly decreased hydrogen concentration.

2.3 Kinetics of dark and photoerasure

It is important to note that the very small values of η^s for TM$_2$ modes cannot be attributed to a high dark conductivity of the

regions in which these modes are travelling. This conclusion is corroborated when we compare the time constant τ of optical erasure (3) and the time constant τ_d of hologram decay in the dark; a relation $\tau \ll \tau_d$ is fulfilled in all our annealed copper-doped samples for TM$_2$, TM$_3$ and TM$_4$ modes. The measurements of τ_d and τ allow us to determine dark- and photo-conductivity (σ_d and σ_{ph}, respectively). From a comparison of different modes in all waveguides we obtain

$$\sigma_d(TM_2) > \sigma_d(TM_3) \geq \sigma_d(TM_4) \leq 10^{16} \,[\Omega\,\text{cm}]^{-1} . \tag{6}$$

We deduce the photoconductivity σ_{ph} from experimental data of τ and τ_d. Because of $\tau_d \gg \tau$, we obtain values of σ_{ph} ranging from 10^{-15} to 5×10^{-13} (Ω cm)$^{-1}$ under our experimental conditions. In [12] the dark-conductivity values between 2×10^{-15} and 2×10^{-14} (Ω cm)$^{-1}$ were reported for single-mode proton-exchanged LiTaO$_3$ waveguides annealed for 1–2 hours at $325\,^\circ$C $- 350\,^\circ$C. Here the hydrogen concentration x at the propagation depth of the TM$_0$ mode is much larger than x for the TM$_2$, TM$_3$ and TM$_4$ modes in our waveguides.

For our waveguides we always observe a pronounced minimum of η^s for an annealing time of 2 hours. For this annealing time we measure a decrease in the transparency of our samples by a factor larger than 3, independent of the lasers wavelength. This behaviour agrees with results of [8]. Optical losses increase sharply at intermediate annealing times because of light scattering at inhomogeneities of composition. For this range crystal regrowth occurs in the proton-exchanged layer at the transition from the β- to the α-phase, and in the near-surface part of the waveguide a region with intermixed small grains of two phases appears.

We also study the kinetics of optical erasure in holographic gratings as a function of the input power P_{in}. At low values of P_{in} the time constant τ is inversely proportional to P_{in} for all TM$_i$ modes with $i \geq 2$, see Fig. 3. At higher input powers deviations from this relation between τ and P_{in} are observed: The measured time constants are smaller than the values extrapolated from the curve at low P_{in}, which means
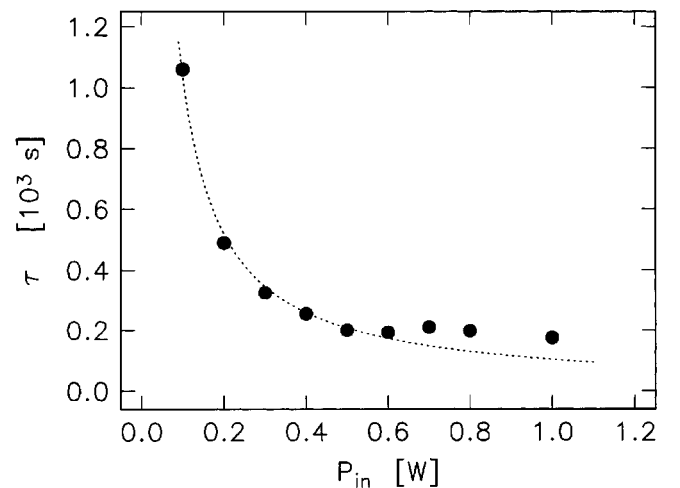
Fig. 3. Time constant τ of photoerasure versus input power P_{in} for the waveguide LT2 annealed for 1 h at $350\,^\circ$C. The experimental data ($\bullet$ measuring uncertainties $\pm 10\%$) are obtained for the TM$_4$ mode at $\lambda_0 = 488$ nm. The *dashed line* is the dependence $\tau P_{in} = $ const. with the value of τ taken at $P_{in} = 0.1$ W

that the relation $\tau P_{\text{in}} = $ const. is not fulfilled. This behaviour of τ is the result of photoinduced light scattering or fanning of the guided light. To determine this beam fanning, the ratio f of output to input power is measured as a function of input power, $f(P_{\text{in}}) = P_{\text{out}}/P_{\text{in}}$. We observe a decrease of the ratio f at high input powers P_{in}, which correlates with the anomalous behaviour of the time constant τ. Fanning only appears beyond a certain threshold value of P_{in}. This threshold behaviour of fanning is in agreement with the data of previous investigations [13, 14]. The threshold value is found to be inversely proportional to the copper content and increases with increasing hydrogen concentration. In extreme cases fanning completely suppresses holographic recording. However, at low P_{in} values fanning is absent and, therefore, the light intensity I in the waveguide is proportional to P_{in}. Thus we can write $(\tau P_{\text{in}})^{-1} \sim \sigma_{\text{ph}}/P_{\text{in}} \sim \kappa\sigma^{\text{spec}}$, where κ is the absorption coefficient and σ^{spec} is the specific photoconductivity. The experimental values of $(\tau P_{\text{in}})^{-1}$ at low P_{in} yields information for the comparison of different modes of different waveguides. The absorption coefficient can be split into two contributions, $\kappa = \kappa_{\text{S}} + \kappa_{\text{Cu}}$, where κ_{S} is the absorption coefficient of the substrate and κ_{Cu} is the coefficient of the absorption which is induced by the copper exchange. Hence, we can use the values of $(\tau P_{\text{in}})^{-1}$ (Table 3) for the determination of the relative changes of the copper concentration C_{Cu} in the waveguide:

$$C_{\text{Cu}} \sim \kappa_{\text{Cu}} \sim (\tau_{\text{Cu}} P_{\text{in}})^{-1} - (\tau_{\text{u}} P_{\text{in}})^{-1}, \tag{7}$$

where τ_{Cu} and τ_{u} are the time constants of the copper-doped and the undoped waveguides, respectively. Note, that this relation may be only used for the comparison of waveguides with similar optical losses.

The changes of C_{Cu} derived from (7) agree with data of the optical absorption spectra shown in Fig. 1, as well as with copper-induced changes of δn_{e} in Table 1. Moreover, these results demonstrate a strong increase of the copper-induced absorption κ_{Cu} for the TM_2, TM_3 and TM_4 modes in the waveguides annealed for 6 hours at 350 °C (Table 3). This clearly indicates the blurring of the copper profile in the waveguides caused by strong annealing. Consequently, these data also show that the changes of σ_{ph} for a variation of P_{in} depend on the annealing time t_{a}. At $t_{\text{a}} = 1$ and 3 hours the values of σ_{ph} range from 3×10^{-15} to 10^{-13} $(\Omega\,\text{cm})^{-1}$, at $t_{\text{a}} = 2$ hours from 10^{-15} to 5×10^{-14} $(\Omega\,\text{cm})^{-1}$, and at $t_{\text{a}} = 6$ hours from 2×10^{-14} to 5×10^{-13} $(\Omega\,\text{cm})^{-1}$. Note, that the upper value

Table 3. Experimental values of $(\tau P_{\text{in}})^{-1}$ [in 10^{-3} $(\text{W}\,\text{s})^{-1}$] in different waveguides (measuring accuracy $\pm 10\%$)

Modes	waveguides					
	LT1		LT2			LT4
				t_{a} [h]		
	1	1	2	3	6	1
TM_4	4	9	3	10	69	100
TM_3	*	22	14	33	273	**
TM_2	*	*	*	51	490	*

*holographic recording and erasure could not be observed;
**strong fanning is observed even at the lowest value of input power P_{in} of 0.015 W

of σ_{ph} is limited by beam fanning, and this effect is strongest for waveguides annealed for 6 hours. A simple approximation using the power coupled out of the waveguide gives a total intensity $I \leq 100$ W cm^{-2} inside the waveguides for an input power of $P_{\text{in}} = 1.0$ W.

2.4 Holographic sensitivity

In the region where the light intensity I in the waveguide is proportional to the input power P_{in}, we can compare the photorefractive sensitivity S of different modes in different waveguides. The photorefractive sensitivity S is defined as

$$S = \text{d}(\Delta n_{\text{e}})/\text{d}(It)|_{t \to 0}, \tag{8}$$

where Δn_{e} is the light-induced extraordinary index change.

However, a direct quantitative determination of S is not possible as the value of intensity depends on several experimental parameters (coupling coefficient for the prism-waveguide boundary, beam diameter in the waveguide, etc.) which we cannot measure precisely.

To compare modes of different samples, we determine the value of the holographic sensitivity R from the rate of hologram build-up in the initial stage:

$$R = \text{d}(\sqrt{\eta})/\text{d}(P_{\text{in}}t)|_{t \to 0}. \tag{9}$$

Evidently, S is proportional to R in the region where the ratio $f = P_{\text{out}}/P_{\text{in}}$ is constant.

The measurements point out that R depends strongly on input power P_{in}, (Fig. 4). Thus we write

$$R = R_1 + R_{\text{q}}P_{\text{in}}, \tag{10}$$

and $\quad S = S_1 + S_{\text{q}}I$.

The relations $S_1 \sim R_1$ and $S_{\text{q}} \sim R_{\text{q}}$ are experimentally verified. From the comparison of TM_3 and TM_4 modes of different waveguides we can conclude that the quadratic part of S
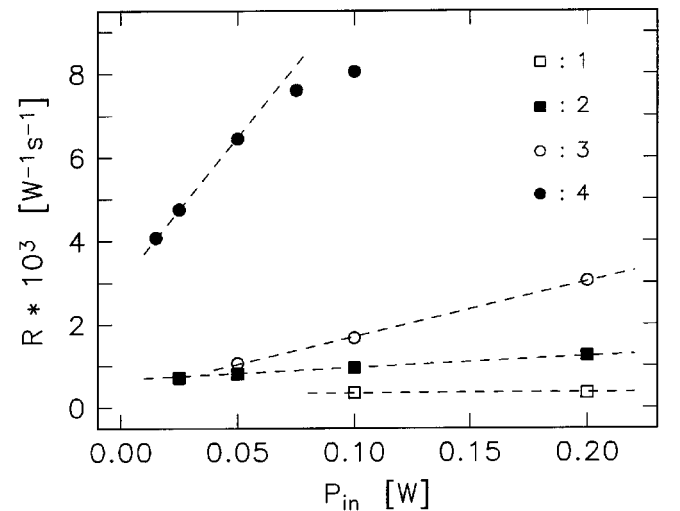
Fig. 4. Holographic sensitivity R versus P_{in} at $\lambda_0 = 488$ nm for different modes and waveguides annealed for 1 hour at 350 °C (measuring accuracy $\pm 15\%$): *1* TM_4 modes in the waveguide LT1; *2* TM_4 modes in the waveguide LT2; *3* TM_3 modes in the waveguide LT2; *4* TM_4 modes in the waveguide LT4

Table 4. Values of the linear part R_1 [in 10^{-3} (W s)$^{-1}$] and the quadratic part R_q [in 10^{-3} (W s)$^{-1}$] of the holographic sensitivity R (measuring accuracy about $\pm15\%$) in different waveguides annealed for 1 h at 350 °C

waveguides	modes			
	TM$_4$		TM$_3$	
	R_1	R_q	R_1	R_q
LT1	0.35	0	*	*
LT2	0.65	0.30	0.37	1.7
LT4	3.10	6.70	**	**

*holographic recording and erasure could not be observed;
**strong fanning for any values of input power P_{in}

is almost proportional to the copper-induced absorption (i.e. proportional to C_{Cu}) which is derived from (7) and the experimental values of τ, see Table 4. A deviation from such a proportionality and very small values of R_q are found for TM$_2$ modes (although the value of κ_{Cu} is increased compared with that for TM$_3$ and TM$_4$ modes). This is caused by the influence of different phases. The (5) and (9)–(10) yield:

$$S_q \sim R_q \sim C_{Cu}(x_\beta - x)(x_t - x). \tag{11}$$

Consequently, the origins of the intensity dependence of Δn^s for our copper-doped proton-exchanged LiTaO$_3$ waveguides and the undoped annealed proton-exchanged LiNbO$_3$ waveguides of [11] are different. In these LiNbO$_3$ waveguides the change of Δn^s is mainly a result of the high dark-conductivity. In our LiTaO$_3$ waveguides, however, the intensity dependence of diffraction efficiency may be explained by considering an additional photorefractive center and a two-center model for the photoinduced charge transport [15]. A significant role of intrinsic defects in LiTaO$_3$ has to be assumed for the explanation of the charge transport in our copper-doped waveguides.

3 Conclusions

By an additional copper exchange, the photorefractive properties of annealed proton-exchanged LiTaO$_3$ waveguides are considerably improved. The steady-state value of diffraction efficiency of holographic gratings in our waveguides is increased from 0.005% to 6%. It is established, that there is a strong difference between different TM modes concerning magnitude and kinetics of the photorefractive response. This points to a crucial influence of the phase of the waveguiding layer that depends on the propagation depth of a mode. The photorefractive sensitivity S is a function of light intensity and the intensity dependent part of S correlates with the copper content. Our results also indicate that further improvements should be possible by varying the fabrication conditions.

References

1. T. Findakly, P. Suchoski, F. Leonberger: Opt. Lett. **13**, 797 (1988)
2. A. Donaldson: J. Phys. D **24**, 785 (1991)
3. D. Kip, T. Bartholomäus, P.M. Garcia, E. Krätzig: J. Opt. Soc. Am. B **11**, 1736 (1994)
4. S.M. Kostritskii, O.M. Kolesnikov: J. Opt. Soc. Am. B **11**, 1674 (1994)
5. F. Rickermann, D. Kip, B. Gather, E. Krätzig: Phys. Stat. Sol. (a) **150**, 763 (1995)
6. C.C. Ziling, V.V. Atuchin, I. Savatinova, M. Kuneva: Int. J. Optoelectron. **7**, 519 (1992)
7. Yu. Bobrov, V.A. Ganshin, V.Sh. Ivanov, Yu.N. Korkishko, T.V. Morozova: Phys. Stat. Sol. (a) **123**, 317 (1991)
8. H. Ahlfeldt, J. Webjörm, P.A. Thomas, S.J. Teat: J. Appl. Phys. **77**, 4467 (1995)
9. V.V. Atuchin, S.M. Kostritskii: Optoelectr. Instrum. & Dat. Proces. (Allerton Press Inc.) to be published
10. D. Kip, F. Rickermann, E. Krätzig: Opt. Lett. **20**, 1139 (1995)
11. T. Furukawa, R. Srivastava, X. Cao, R.V. Ramaswamy: Opt. Lett. **18**, 346 (1993)
12. M.M. Howerton, W.K. Burns: J. Lightwave Technol. **10**, 142 (1992)
13. J.-J. Liu, P.P. Banerjee, Q. Wang Song: J. Opt. Soc. Am. B **11**, 1688 (1994)
14. A.A. Kamshilin, B. Raita, A.V. Khomenko: J. Opt. Soc. Am. B **13**, 2536 (1996)
15. F. Jermann, J. Otten: J. Opt. Soc. Am. B **10**, 2085 (1993)